

2

ateri l or phenomena

1, 280–294

July 10, 2019 © 2019 Elsevier Inc.

<https://doi.org/10.1016/j.matt.2019.05.014>



Ar

Spontaneous Non-stoichiometry and Ordering in Degenerate but Gapped Transparent Conductors

Oleksandr I. Malyi,^{1,2,*} Michael T. Yeung,³ Kenneth R. Poeppelmeier,³ Clas Persson,² and Alex Zunger^{1,4,*}

SUMMARY



in [Figure 1B](#)) and then attempting heavy doping (by Sn or Al, respectively), making it

Figure 3.5. Vacancy formation energy in GaIn as a function of the metal chemical potential. The allowed stable chemical potential regions (constructed by considering possible competing phases, see Experimental Procedures) of the respective bulk compounds are shown in Figures 3B, 3D, and 3F. We see that for the degenerate gapped compounds under cation-deficient chemical potential conditions, vacancy formation energies can be extremely low (in fact, negative). Whereas BaNbO₃ and Ca₆Al₇O₁₆ have stable chemical potential (green) zones at the respective stoichiometries indicated, Ag₃Al₂₂O₃₄ does not. In fact, in the latter case, the Ag vacancy formation energy (Figure 3E) is so strongly negative under all chemical potential conditions, that the CB is empty and the parent degenerate Ag₃Al₂₂O₃₄ phase is not stable (i.e., no green zone in Figure 3F).

Detailed description of Figure 3.5: This figure is a plot showing the vacancy formation energy (in eV) on the y-axis versus the metal chemical potential (in eV) on the x-axis for GaIn. The plot is divided into several regions representing different chemical potentials. A green shaded region indicates the stable chemical potential zone for the respective stoichiometries. The plot shows that for the degenerate gapped compounds under cation-deficient chemical potential conditions, vacancy formation energies can be extremely low (in fact, negative). Whereas BaNbO₃ and Ca₆Al₇O₁₆ have stable chemical potential (green) zones at the respective stoichiometries indicated, Ag₃Al₂₂O₃₄ does not. In fact, in the latter case, the Ag vacancy formation energy (Figure 3E) is so strongly negative under all chemical potential conditions, that the CB is empty and the parent degenerate Ag₃Al₂₂O₃₄ phase is not stable (i.e., no green zone in Figure 3F).

Detailed description of Figure 3.6: This figure is a plot showing the vacancy formation energy (in eV) on the y-axis versus the metal chemical potential (in eV) on the x-axis for GaIn. The plot is divided into several regions representing different chemical potentials. A green shaded region indicates the stable chemical potential zone for the respective stoichiometries. The plot shows that for the degenerate gapped compounds under cation-deficient chemical potential conditions, vacancy formation energies can be extremely low (in fact, negative). Whereas BaNbO₃ and Ca₆Al₇O₁₆ have stable chemical potential (green) zones at the respective stoichiometries indicated, Ag₃Al₂₂O₃₄ does not. In fact, in the latter case, the Ag vacancy formation energy (Figure 3E) is so strongly negative under all chemical potential conditions, that the CB is empty and the parent degenerate Ag₃Al₂₂O₃₄ phase is not stable (i.e., no green zone in Figure 3F).

The negative formation energies of dilute vacancies open the possibility of vacancy condensation and long-range ordering (Figure 2B). To examine this possibility, we have calculated the $T = 0$ K stable phases (“ground state diagram” or “convex

hull") of such ternary structures. This entails searching for configuration versus composition that lies on the energy convex hull,¹⁴ which defines the phases with energy lower than a linear combination of any competing phases at the corresponding compositions. We create candidate configurations by considering a base compound (BaNbO_3 , $\text{Ba}_3\text{Nb}_5\text{O}_{15}$, $\text{Ca}_6\text{Al}_7\text{O}_{16}$, or $\text{Ag}_3\text{Al}_{22}\text{O}_{34}$), then create a replica of N such units of the base compound and add successively p metal vacancies, i.e., $\text{OVC} = N \times (\text{base}) + pV_m$, searching via total energy minimization for stable and metastable configurations. We also include experimentally known reconstructed OVCs, the compounds that satisfy the OVC expression but do not have clearly defined vacancy sites (e.g., $\text{Ba}_3\text{Nb}_5\text{O}_{15}$, BaNb_2O_6 , and $\text{Ba}_5\text{Nb}_4\text{O}_6$).

Available information on the experimental literature¹⁵⁻³⁰ is provided in [Figure 4](#), and the theoretical results of this work are summarized in [Figure 5](#). The key point to

and 7B) demonstrating the phases that are stabilized as the chemical potentials of the atoms being removed are continuously changed between their allowed values. Finally, we show how a window of opportunity can be determined computationally between opposing tendencies of (1) stability (Figures 2A and 7B), (2) conductivity (Figures 6B–6D and 7C), and (3) transparency (Figure 8) to design new TCs.

Stable Phases and OVCs for the Ba-Nb-O System

Computationally, we find 25 binary and ternary ground state compounds (described in Data S1) of which $\text{Ba}_7\text{Nb}_6\text{O}_{21}$, $\text{Ba}_5\text{Nb}_4\text{O}_{15}$, $\text{Ba}_3\text{Nb}_5\text{O}_{15}$, $\text{Ba}_7\text{Nb}_8\text{O}_{24}$, $\text{Ba}_9\text{Nb}_{10}\text{O}_{30}$, $\text{Ba}_{26}\text{Nb}_{27}\text{O}_{81}$, and BaNb_2O_6 are OVCs (Figure 5). Here, 7:8:24, 9:10:30, and 26:27:82 phases have clearly defined vacancy sites, and 1:2:6, 3:5:15, and 5:4:15 OVCs are

excluded."¹⁸ Indeed, several potential experimental compositions (i.e., $\text{Ba}_{0.95}\text{NbO}_3$ and $\text{Ba}_{0.97}\text{NbO}_3$) nearly match predicted phases ($\text{Ba}_{26}\text{Nb}_{27}\text{O}_{81}$ Ba

unstable with respect to competing phases. Our experimental attempts to reduce synthesized $\text{Ag}_3\text{Al}_{22}\text{O}_{34.5}$ to $\text{Ag}_3\text{Al}_{22}\text{O}_{34}$

complexity of material synthesis. In our own work on 3:5:15 OVC, we see the preferential formation of the secondary reconstructed 1:2:6 and 5:4:15 OVCs over the targeted compound ([Note S2](#)). This reflects the narrow stability region of the 3:5:15 phase versus the reconstructed OVCs. Hence

frequency but also changes the interband transition, which is illustrated in the absorption spectra of 6:7:16 and its OVCs (see [Figure 8](#)

acceptor states. As a result, the negative electron-hole recombination energy offsets the positive energy associated with vacancy bond breaking. Our results thus explain

$40 \times 40 \times 40$, $20 \times 20 \times 20$, $20 \times 20 \times 20$, $8 \times 24 \times 8$, $16 \times 12 \times 8$, $20 \times 20 \times 20$, $8 \times 8 \times 8$, and $8 \times 8 \times 8$ Γ -centered k-point grids were used for BaNbO_3 , $\text{Ba}_7\text{Nb}_8\text{O}_{24}$, $\text{Ba}_7\text{Nb}_6\text{O}_{21}$, $\text{Ba}_3\text{Nb}_5\text{O}_{15}$, BaNb_2O_6 , $\text{Ca}_6\text{Al}_7\text{O}_{16}$, $\text{Ca}_{23}\text{Al}_{28}\text{O}_{64}$, and $\text{Ca}_{11}\text{Al}_{14}\text{O}_{32}$, respectively. The Drude contribution to optical properties was included by utilizing kram code⁴⁸ with plasma frequencies calculated from first-principles calculations and the damping coefficient of 0.2 eV, which is analogous to traditional TCs.⁴⁹

D C a a n

Supercells with 116, 135, and 236 atoms were used to calculate defect energetics in $\text{Ca}_6\text{Al}_7\text{O}_{16}$, BaNbO_3 , and $\text{Ag}_3\text{Al}_{22}\text{O}_{34}$ systems, respectively. The defect formation energies (Figures 3A, 3C, and 3E) and finite size corrections were computed within the framework described by Lany and Zunger^{50,51} and implemented in the pylada-defects code.⁵² For the defect calculations, the ranges of chemical potentials were determined using only experimentally known stoichiometric crystal structures as described above. It should be noted that unlike conventional insulators where the Fermi energy can span the full range of the gap (Figure 1B), thus controlling the balance between different charges, if the Fermi energy resides inside a continuum band, as is the case in Figure 1A, it represents the energy to add or remove an electron from the host system, not from point defects in the gap. Thus, the conventional calculation of charged defects versus E_F is not meaningful in degenerate gapped materials.

DATA AND SOFTWARE AVAILABILITY

All data needed to evaluate the conclusions in the paper are present in the paper and the Supplemental Information. Additional data related to this paper may be requested from the authors.

SUPPLEMENTAL INFORMATION

Supplemental Information can be found online at <https://doi.org/10.1016/j.matt.2019.05.014>.

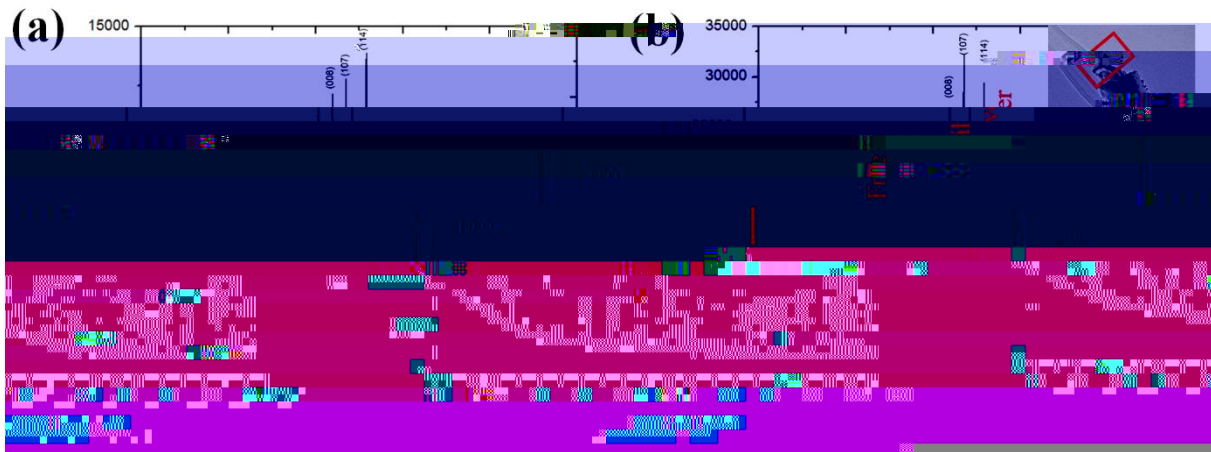
ACKNOWLEDGMENTS

The work of A.Z. and O.I.M. at University of Colorado Boulder, and of K.R.P. and M.T.Y. at Northwestern University, was supported by the NSF-DMR EPM program under grants DMR-1806939 and DMR-1806912, respectively. M.T.Y. would like to thank the Department of Energy (DOE) Office of Energy Efficiency and Renewable Energy (EERE) Postdoctoral Research Award under the EERE Solar Energy Technologies Office administered by the Oak Ridge Institute for Science and Education (ORISE) for the DOE. The ORISE is managed by Oak Ridge Associated Universities (ORAU) under DOE contract number DE-SC00014664. All opinions expressed in this paper are the authors' and do not necessarily reflect the policies and views of DOE, ORAU, or ORISE. O.I.M. and C.P. acknowledge support from the Research Council of Norway (contract no. 251131), and the Norwegian Metacenter for Computational Science (NOTUR) for providing access to supercomputer resources. We would like to thank Zachary Mansley for help with transmission electron microscopy.

AUTHOR CONTRIBUTIONS

O.I.M. carried out the theoretical calculations. M.T.Y. fabricated the samples and carried out structure analysis by X-ray powder diffraction. A.Z. directed the design of the research, analysis of the results, and writing of the paper. O.I.M. contributed most to writing of the paper, with contributions from all co-authors. K.R.P. supervised the experimental work. C.P. and A.Z. supervised all theoretical studies.

39. Dalpian, G.M., Liu, Q., Varignon, J., Bibes, M., and Zunger, A. (2018). Bond disproportionation, charge self-regulation, and ligand holes in ABX_3 perovskites by density functional theory. *Phys. Rev. B* 98, 075135.
40. Liu, Q., Dalpian, G.M., and Zunger, A. (2019). Antidoping in insulators and semiconductors having intermediate bands with trapped carriers. *Phys. Rev. Lett.* 122, 106403.
41. Monkhorst, H.J., and Pack, J.D. (1976). Special points for Brillouin-zone integrations. *Phys. Rev. B* 13, 5188–5192.
42. Momma, K., and Izumi, F. (2011). VESTA 3 for three-dimensional visualization of crystal, volumetric and morphology data. *J. Appl. Crystallogr.* 44, 1272–1276.
43. Ong, S.P., Richards, W.D., Jain, A., Hautier, G., Kocher, M., Cholia, S., Gunter, D., Chevrier, V.L., Persson, K.A., and Ceder, G. (2013). Python Materials Genomics (pymatgen): a robust, open-source python library for materials analysis. *Comp. Mater. Sci.* 68, 314–319.
44. SpringerMaterials, The Landolt–Bornstein Database.



Ag formation in $\text{Ag}_3\text{Al}_{22}\text{O}_{34+x}$ under reduced atmosphere. (a) The powder X-ray diffraction of $\text{Ag}_3\text{Al}_{22}\text{O}_{34.5}$ can be indexed to the JCPDS reference pattern #01-084-0514, corresponding with the phase " $\text{Ag}_3\text{Al}_{22}\text{O}_{34}$ " identified by Tofield³. (b) Any attempts to reduce $\text{Ag}_3\text{Al}_{22}\text{O}_{34.5}$ and introduce carriers results in the precipitation of free metallic silver and the possible formation of $\text{Ag}_{2.5}\text{Al}_{22}\text{O}_{34.25}$.

Ba

_symmetry_space_group_name_H-M 'P 1'
_cell_length_a 4.35636765
_cell_length_b 4.35636704
_cell_length_c 4.35636800
_cell_angle_alpha 109.47121581

BaO

_symmetry_space_group_name_H-M 'P 1'

_cell_length_a 5.61544600

_cell_length_b 5.61562200

_cell_length_c 5.61599000

BaO₂

_symmetry_space_group_name_H-M 'P 1'
_cell_length_a 4.43253442
_cell_length_b 4.43253442
_cell_length_c 7.72989432
_cell_angle_alpha 64.10308353
_cell_angle_beta 64.10308353
_cell_angle_gamma 51.68671041
_symmetry_Int_Tables_number 1
_chemical_formula_structural BaO2
_chemical_formula_sum 'Ba2 O4'
_cell_volume 104.19138075
_cell_formula_units_Z 2
loop_
_symmetry_equiv_pos_site_id
_symmetry_equiv_pos_as_xyz
1 'x, y, z'
loop_
_atom_site_type_symbol
_atom_site_label
_atom_site_symmetry_multiplicity
_atom_site_fract_x
_atom_site_fract_y
_atom_site_fract_z
_atom_site_occupancy
Ba Ba1 1 0.500535 0.499465 0.250000 1
Ba Ba2 1 0.499465 0.500535 0.750000 1
O O3 1 0.888579 0.895978 0.054472 1
O O4 1 0.104022 0.111421 0.445528 1
O O5 1 0.111421 0.104022 0.945528 1
O O6 1 0.895978 0.888579 0.554472 1

Nb

_symmetry_space_group_name_H-M 'P 1'
_cell_length_a 2.90286990
_cell_length_b 2.90286979
_cell_length_c 2.90286989
_cell_angle_alpha 109.47120777
_cell_angle_beta 109.47120700
_cell_angle_gamma 109.47123504
_symmetry_Int_Tables_number 1
_chemical_formula_structural Nb
_chemical_formula_sum Nb1
_cell_volume 18.83045752
_cell_formula_units_Z 1
loop_
_symmetry_equiv_pos_site_id
_symmetry_equiv_pos_as_xyz
1 'x, y, z'
loop_
_atom_site_type_symbol
_atom_site_label
_atom_site_symmetry_multiplicity
_atom_site_fract_x
_atom_site_fract_y
_atom_site_fract_z

Nb₈O

```
_symmetry_space_group_name_H-M 'P 1'  
_cell_length_a 3.33819808  
_cell_length_b 9.70864476  
_cell_length_c 9.70054127  
_cell_angle_alpha 89.94499925  
_cell_angle_beta 89.99641670  
_cell_angle_gamma 89.99435529  
_symmetry_Int_Tables_number 1  
_chemical_formula_structural Nb8O  
_chemical_formula_sum 'Nb16 O2'  
_cell_volume 314.38837414  
_cell_formula_units_Z 2  
loop_  
_symmetry_equiv_pos_site_id  
_symmetry_equiv_pos_as_xyz  
1 'x, y, z'  
loop_  
_atom_site_type_symbol  
_atom_site_label  
_atom_site_symmetry_multiplicity  
_atom_site_fract_x  
_atom_site_fract_y  
_atom_site_fract_z  
_atom_site_occupancy  
Nb Nb1 1 0.502301 0.127693 0.383456 1  
Nb Nb2 1 0.502376 0.868509 0.616799 1  
Nb Nb3 1 0.002331 0.627667 0.116797 1  
Nb Nb4 1 0.002086 0.368558 0.883454 1  
Nb Nb5 1 0.502211 0.381333 0.129773 1  
Nb Nb6 1 0.502231 0.614875 0.870486 1  
Nb Nb7 1 0.002441 0.114851 0.629711 1  
Nb Nb8 1 0.002202 0.881324 0.370550 1  
Nb Nb9 1 0.501894 0.651434 0.346653 1  
Nb Nb10 1 0.501875 0.344707 0.653627 1  
Nb Nb11 1 0.002629 0.151361 0.153523 1  
Nb Nb12 1 0.002765 0.844838 0.846713 1  
Nb Nb13 1 0.502983 0.880124 0.118046 1  
Nb Nb14 1 0.502987 0.116100 0.882237 1  
Nb Nb15 1 0.001753 0.380053 0.382178 1  
Nb Nb16 1 0.001461 0.616152 0.618093 1  
O O17 1 0.501405 0.498093 0.500170 1  
O O18 1 0.003083 0.998097 0.000129 1
```

Nb₁₂O₂₉

_symmetry_space_group_name_H-M 'P 1'
_cell_length_a 10.76552232
_cell_length_b 10.76552083
_cell_length_c 29.49183109
_cell_angle_alpha 89.99362541

Nb Nb23 1 0.648180 0.351357 0.315624 1
Nb Nb24 1 0.352774 0.648138 0.684530 1
O O25 1 0.454811 0.538502 0.250094 1
O O26 1 0.538262 0.452974 0.750090 1
O O27 1 0.832029 0.161325 0.250066 1
O O28 1 0.161138 0.830145 0.750093 1
O O29 1 0.649067 0.346411 0.250103 1
O O30 1 0.345526 0.646439 0.750057 1

NbO₂

_symmetry_space_group_name_H-M 'P 1'
_cell_length_a 6.07119815
_cell_length_b 9.87925843
_cell_length_c 9.87701218
_cell_angle_alpha 90.00173369
_cell_angle_beta 90.00746424
_cell_angle_gamma 90.00302134
_symmetry_Int_Tables_number 1
_chemical_formula_structural NbO2
_chemical_formula_sum 'Nb16 O32'
_cell_volume 592.41267097
_cell_formula_units_Z 16
loop_
_symmetry_equiv_pos_site_id
_symmetry_equiv_pos_as_xyz
1 'x, y, z'
loop_
_atom_site_type_symbol
_atom_site_label
_atom_site_symmetry_multiplicity
_atom_site_fract_x
_atom_site_fract_y
_atom_site_fract_z
_atom_site_occupancy

O 023 1 0.491071 0.099715 0.653686 1
O 024 1 0.491115 0.897280 0.350364 1
O 025 1 0.756096 0.362104 0.611880 1
O 026 1 0.756078 0.635087 0.392008 1
O 027 1 0.006150 0.888958 0.365898 1
O 028 1 0.006125 0.108100 0.638169 1
O 029 1 0.256071 0.862216 0.111769 1
O 030 1 0.255937 0.134902 0.892191 1
O 031 1 0.506085 0.388753 0.865734 1
O 032 1 0.505954 0.608185 0.138238 1
O 033 1 0.236968 0.362047 0.111990 1
O 034 1 0.236980 0.634862 0.892207 1
O 035 1 0.487004 0.388982 0.365957 1
O 036 1 0.486886 0.608057 0.638125 1
O 037 1 0.736760 0.862152 0.611815 1
O 038 1 0.736735 0.134877 0.392233 1
O 039 1 0.986987 0.888783 0.865719 1
O 040 1 0.986995 0.108172 0.138254 1
O 041 1 0.501930 0.099700 0.153588 1
O 042 1 0.501896 0.897331 0.850414 1
O 043 1 0.751882 0.346835 0.103318 1
O 044 1 0.751779 0.650199 0.900709 1
O 045 1 0.001783 0.599713 0.653569 1
O 046 1 0.001784 0.397365 0.350534 1
O 047 1 0.251897 0.846721 0.603355 1
O 048 1 0.251917 0.150367 0.400629 1

NbO

_symmetry_space_group_name_H-M 'P 1'
_cell_length_a 4.28364712
_cell_length_b 4.28323117
_cell_length_c 4.28269574
_cell_angle_alpha 90.02163794
_cell_angle_beta 90.02487418
_cell_angle_gamma 89.97714155
_symmetry_Int_Tables_number 1
_chemical_formula_structural NbO
_chemical_formula_sum 'Nb3 O3'
_cell_volume 78.57824324
_cell_formula_units_Z 3
loop_
_symmetry_equiv_pos_site_id
_symmetry_equiv_pos_as_xyz
1 'x, y, z'
loop_
_atom_site_type_symbol
_atom_site_label
_atom_site_symmetry_multiplicity
_atom_site_fract_x
_atom_site_fract_y
_atom_site_fract_z
_atom_site_occupancy
Nb Nb1 1 0.505882 0.994045 0.500982 1
Nb Nb2 1 0.505847 0.494398 0.000883 1
Nb Nb3 1 0.005871 0.494443 0.501004 1
O O4 1 0.005984 0.994384 0.501149 1
O O5 1 0.506078 0.994360 0.001096 1
O O6 1 0.005938 0.493956 0.001060 1

Nb₂O₅

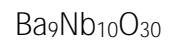
_symmetry_space_group_name_H-M 'P 1'
_cell_length_a 3.89190501
_cell_length_b 19.79300144
_cell_length_c 20.82946079
_cell_angle_alpha 64.37219889
_cell_angle_beta 90.00103500
_cell_angle_gamma 90.00214144
_symmetry_Int_Tables_number 1
_chemical_formula_structural Nb2O5
_chemical_formula_sum 'Nb28 O70'
_cell_volume 1446.69434171
_cell_formula_units_Z 14
loop_
_symmetry_equiv_pos_site_id
_symmetry_equiv_pos_as_xyz
1 'x, y, z'
loop_
_atom_site_type_symbol
_atom_site_label
_atom_site_symmetry_multiplicity
_atom_site_fract_x
_atom_site_fract_y
_atom_site_fract_z
_atom_site_occupancy
Nb Nb1 1 0.989629 0.160998 0.834128 1
Nb Nb2 1 0.498987 0.421155 0.703005 1
Nb Nb3 1 0.005453 0.004647 0.763546 1
Nb Nb4 1 0.984459 0.156122 0.566579 1
Nb Nb5 1 0.001231 0.693061 0.628814 1
Nb Nb6 1 0.004717 0.995881 0.235761 1
Nb Nb7 1 0.998223 0.152055 0.302579 1
Nb Nb8 1 0.498459 0.734115 0.839873 1
Nb Nb9 1 0.999145 0.316040 0.638360 1
Nb Nb10 1 0.999282 0.684483 0.360997 1
Nb Nb11 1 0.998396 0.848526 0.696649 1
Nb Nb12 1 0.998945 0.531305 0.562205 1
Nb Nb13 1 0.509791 0.110158 0.093378 1
Nb Nb14 1 0.499428 0.580409 0.770062 1
Nb Nb15 1 0.494823 0.264543 0.898402 1
Nb Nb16 1 0.524979 0.424311 0.964523 1
Nb Nb17 1 0.498679 0.579400 0.296328 1
Nb Nb18 1 0.026399 0.000297 0.499620 1
Nb Nb19 1 0.230222 0.000228 0.999650 1
Nb Nb20 1 0.510444 0.890377 0.905938 1
Nb Nb21 1 0.998776 0.469211 0.437128 1
Nb Nb22 1 0.984298 0.844413 0.432737 1

O 070 1 0.995534 0.914039 0.195169 1
O 071 1 0.996472 0.086485 0.804171 1
O 072 1 0.498953 0.501014 0.272165 1

O 023 1 0.002169 0.749996 0.755711 1
O 024 1 0.248539 0.253625 0.005544 1
O 025 1 0.252281 0.249588 0.505538 1
O 026 1 0.248412 0.746074 0.005525 1
O 027 1 0.252495 0.750109 0.505533 1
O 028 1 0.755781 0.253719 0.005523 1
O 029 1 0.752092 0.249495 0.505519 1
O 030 1 0.755963 0.745978 0.005511 1
O 031 1 0.751916 0.750231 0.505515 1
O 032 1 0.248574 0.999833 0.259258 1
O 033 1 0.248346 0.999841 0.751818 1
O 034 1 0.252332 0.499831 0.255349 1
O 035 1 0.252496 0.499844 0.755727 1
O 036 1 0.755836 0.999850 0.259113 1
O 037 1 0.756002 0.999863 0.751929 1
O 038 1 0.752092 0.499853 0.255439 1
O 039 1 0.751881 0.499858 0.755621 1

Ba Ba23 1 0.999850 0.333520 0.670661 1
Ba Ba24 1 0.999809 0.668282 0.003186 1
Ba Ba25 1 0.999880 0.668330 0.335765 1
Ba Ba26 1 0.999880 0.668363 0.670635 1
Nb Nb27 1 0.167677 0.700167 0.4990008871 0 595.32 841.92 reWⁿBT/F1 12 Tf1 0 0 1 277.85 714.58 TmC

O 0117 1 0.501951 0.000884 0.172673 1
O 0118 1 0.499254 0.000913 0.503163 1
O 0119 1 0.501973 0.000920 0.833592 1
O 0120 1 0.499018 0.334114 0.169756 1



O 023 1 0.949491 0.399829 0.749274 1
O 024 1 0.694372 0.898841 0.000152 1
O 025 1 0.799430 0.100308 0.499949 1
O 026 1 0.649550 0.300400 0.749846 1
O 027 1 0.948548 0.898497 0.254504 1
O 028 1 0.649241 0.800126 0.250010 1
O 029 1 0.745803 0.000444 0.746212 1
O 030 1 0.599521 0.700225 0.499974 1
O 031 1 0.499722 0.499932 0.999784 1
O 032 1 0.449792 0.900031 0.749829 1
O 033 1 0.749549 0.500426 0.250001 1
O 034 1 0.449866 0.399685 0.249370 1
O 035 1 0.549318 0.600288 0.750191 1
O 036 1 0.304851 0.101130 0.999421 1
O 037 1 0.399448 0.299779 0.499587 1
O 038 1 0.249713 0.499679 0.749848 1
O 039 1 0.549381 0.099951 0.249834 1
O 040 1 0.253346 0.999511 0.253291 1
O 041 1 0.349983 0.199847 0.749609 1
O 042 1 0.100611 0.694219 0.999745 1
O 043 1 0.199869 0.899685 0.499649 1
O 044 1 0.050663 0.101495 0.745160 1
O 045 1 0.349615 0.699505 0.249469 1
O 046 1 0.049753 0.600130 0.250316 1
O 047 1 0.152045 0.796380 0.745679 1
O 048 1 0.999696 0.499919 0.499805 1
O 049 1 0.152319 0.304752 0.253419 1

Ba₂Nb₅O₉

_symmetry_space_group_name_H-M 'P 1'
_cell_length_a 4.24427900
_cell_length_b 4.24430501
_cell_length_c 12.43007201
_cell_angle_alpha 89.99971548
_cell_angle_beta 89.99578851
_cell_angle_gamma 89.99671969
_symmetry_Int_Tables_number 1
_chemical_formula_structural Ba₂Nb₅O₉
_chemical_formula_sum 'Ba₂ Nb₅ O₉'
_cell_volume 223.91549800
_cell_formula_units_Z 1
loop_
_symmetry_equiv_pos_site_id
_symmetry_equiv_pos_as_xyz
1 'x, y, z'
loop_
_atom_site_type_symbol
_atom_site_label
_atom_site_symmetry_multiplicity
_atom_site_fract_x
_atom_site_fract_y
_atom_site_fract_z
_atom_site_occupancy
Ba Ba1 1 0.004334 0.002399 0.168067 1
Ba Ba2 1 0.004678 0.002242 0.831704 1
Nb Nb3 1 0.504344 0.501894 0.999908 1
Nb Nb4 1 0.504755 0.502639 0.337074 1
Nb Nb5 1 0.504807 0.502589 0.662686 1
Nb Nb6 1 0.004850 0.502827 0.499878 1

BaNb₇O₉

_symmetry_space_group_name_H-M 'P 1'
_cell_length_a 4.26656500
_cell_length_b 4.26679901
_cell_length_c 12.63075502
_cell_angle_alpha 89.99797195
_cell_angle_beta 90.00247263
_cell_angle_gamma 90.00029533
_symmetry_Int_Tables_number 1
_chemical_formula_structural BaNb₇O₉
_chemical_formula_sum 'Ba1 Nb7 O9'
_cell_volume 229.93753073
_cell_formula_units_Z 1
loop_
_symmetry_equiv_pos_site_id
_symmetry_equiv_pos_as_xyz
1 'x, y, z'
loop_
_atom_site_type_symbol
_atom_site_label
_atom_site_symmetry_multiplicity
_atom_site_fract_x
_atom_site_fract_y
_atom_site_fract_z
_atom_site_occupancy
Ba Ba1 1 0.989408 0.005548 0.000030 1
Nb Nb2 1 0.489417 0.505643 0.500013 1
Nb Nb3 1 0.989587 0.505637 0.671313 1
Nb Nb4 1 0.489668 0.005550 0.671329 1
Nb Nb5 1 0.989328 0.505660 0.328693 1
Nb Nb6 1 0.489326 0.005622 0.328683 1
Nb Nb7 1 0.489561 0.505670 0.831492 1
Nb Nb8 1 0.489303 0.505740 0.168512 1
O O9 1 0.489273 0.005634 0.500007 1

Ba₆Nb₂O₁₁

_symmetry_space_group_name_H-M 'P 1'
_cell_length_a 6.29863509
_cell_length_b 6.31021801
_cell_length_c 20.62786560
_cell_angle_alpha 91.04383036
_cell_angle_beta 97.47155254
_cell_angle_gamma 119.74476774
_symmetry_Int_Tables_number 1
_chemical_formula_structural Ba₆Nb₂O₁₁
_chemical_formula_sum 'Ba₁₂ Nb₄ O₂₂'
_cell_volume 702.53673442
_cell_formula_units_Z 2
loop_
_symmetry_equiv_pos_site_id
_symmetry_equiv_pos_as_xyz
1 'x, y, z'
loop_

BaNb₅O₈

_symmetry_space_group_name_H-M 'P 1'
_cell_length_a 4.18373802
_cell_length_b 6.72819011
_cell_length_c 6.72311020
_cell_angle_alpha 89.97578764
_cell_angle_beta 90.00797859
_cell_angle_gamma 90.00314405
_symmetry_Int_Tables_number 1
_chemical_formula_structural BaNb₅O₈
_chemical_formula_sum 'Ba1 Nb5 O8'
_cell_volume 189.24870779
_cell_formula_units_Z 1
loop_
_symmetry_equiv_pos_site_id
_symmetry_equiv_pos_as_xyz
1 'x, y, z'
loop_
_atom_site_type_symbol
_atom_site_label
_atom_site_symmetry_multiplicity
_atom_site_fract_x
_atom_site_fract_y
_atom_site_fract_z
_atom_site_occupancy
Ba Ba1 1 0.999130 0.000273 0.003188 1
Nb Nb2 1 0.499136 0.211862 0.601927 1
Nb Nb3 1 0.499091 0.401540 0.214950 1
Nb Nb4 1 0.999178 0.500264 0.503196 1
Nb Nb5 1 0.499251 0.598962 0.791449 1
Nb Nb6 1 0.499174 0.788648 0.404460 1
O O7 1 0.499052 0.098914 0.304240 1
O O8 1 0.999140 0.204599 0.617098 1
O O9 1 0.499132 0.301272 0.904555 1
O O10 1 0.999098 0.386461 0.207484 1
O O11 1 0.999274 0.614012 0.798938 1
O O12 1 0.499287 0.699209 0.101839 1
O O13 1 0.999187 0.795912 0.389246 1
O O14 1 0.499223 0.901598 0.702172 1

Ba₄Nb₂O₉

_symmetry_space_group_name_H-M 'P 1'
_cell_length_a 6.10372112
_cell_length_b 10.42767657
_cell_length_c 17.19094999
_cell_angle_alpha 90.42508018
_cell_angle_beta 89.99308306
_cell_angle_gamma 89.99778826
_symmetry_Int_Tables_number 1
_chemical_formula_structural Ba₄Nb₂O₉
_chemical_formula_sum 'Ba₁₆ Nb₈ O₃₆'
_cell_volume 1094.13309695
_cell_formula_units_Z 4
loop_
_symmetry_equiv_pos_site_id
_symmetry_equiv_pos_as_xyz
1 'x, y, z'
loop_

O O23 1 0.168870 0.337740 0.191700 1
O O24 1 0.662260 0.831130 0.191700 1

Ba₇Nb₆O₂₁

_symmetry_space_group_name_H-M 'P 1'

_cell_length_a 17.17666038

_cell_length_b 17.17666038

_cell_length_c 17.17666048

_cell_angle_alpha 19.75304374

_cell_angle_beta 19.75304374

_cell_angle_gamma 19.75304487

_symmetry_Int_Tables_number 1

Ba₂Nb₁₅O₃₂

_symmetry_space_group_name_H-M 'P 1'
_cell_length_a 7.92360186
_cell_length_b 7.92024685
_cell_length_c 36.45514839
_cell_angle_alpha 90.48688439
_cell_angle_beta 89.86379007
_cell_angle_gamma 119.87761907
_symmetry_Int_Tables_number 1
_chemical_formula_structural Ba₂Nb₁₅O₃₂
_chemical_formula_sum 'Ba6 Nb45 O96'
_cell_volume 1983.66548680
_cell_formula_units_Z 3
loop_
_symmetry_equiv_pos_site_id
_symmetry_equiv_pos_as_xyz
1 'x, y, z'
loop_
_atom_site_type_symbol
_atom_site_label

BaNb₈O

Nb Nb23	1	0.375709	0.421362	0.433591	1
Nb Nb24	1	0.875709	0.578638	0.066409	1
Nb Nb25	1	0.377054	0.927082	0.182378	1
Nb Nb26	1	0.877054	0.072918	0.317622	1
Nb Nb27	1	0.622946	0.572918	0.682378	1
Nb Nb28	1	0.122946	0.427082	0.817622	1
Nb Nb29	1	0.622946	0.072918	0.817622	1
Nb Nb30	1	0.122946	0.927082	0.682378	1
Nb Nb31	1	0.377054	0.427082	0.317622	1
Nb Nb32	1	0.877054	0.572918	0.182378	1
Nb Nb33	1	0.381809	0.161385	0.120165	1
Nb Nb34	1	0.881809	0.838615	0.379835	1
Nb Nb35	1	0.618191	0.338615	0.620165	1
Nb Nb36	1	0.118191	0.661385	0.879835	1
Nb Nb37	1	0.618191	0.838615	0.879835	1
Nb Nb38	1	0.118191	0.161385	0.620165	1
Nb Nb39	1	0.381809	0.661385	0.379835	1
Nb Nb40	1	0.881809	0.338615	0.120165	1
Nb Nb41	1	0.361827	0.185140	0.253526	1
Nb Nb42	1	0.861827	0.814860	0.246474	1
Nb Nb43	1	0.638173	0.314860	0.753526	1
Nb Nb44	1	0.138173	0.685140	0.746474	1
Nb Nb45	1	0.638173	0.814860	0.746474	1
Nb Nb46	1	0.138173	0.185140	0.753526	1
Nb Nb47	1	0.361827	0.685140	0.246474	1
Nb Nb48	1	0.861827	0.314860	0.253526	1
Nb Nb49	1	0.117159	0.159820	0.998594	1
Nb Nb50	1	0.617159	0.840180	0.501406	1
Nb Nb51	1	0.882841	0.340180	0.498594	1
Nb Nb52	1	0.382841	0.659820	0.001406	1
Nb Nb53	1	0.882841	0.840180	0.001406	1
Nb Nb54	1	0.382841	0.159820	0.498594	1
Nb Nb55	1	0.117159	0.659820	0.501406	1
Nb Nb56	1	0.617159	0.340180	0.998594	1
Nb Nb57	1	0.617001	0.834936	0.124067	1
Nb Nb58	1	0.117001	0.165064	0.375933	1
Nb Nb59	1	0.382999	0.665064	0.624067	1
Nb Nb60	1	0.882999	0.334936	0.875933	1
Nb Nb61	1	0.382999	0.165064	0.875933	1
Nb Nb62	1	0.882999	0.834936	0.624067	1
Nb Nb63	1	0.617001	0.334936	0.375933	1
Nb Nb64	1	0.117001	0.665064	0.124067	1
Nb Nb65	1	0.624232	0.076048	0.182918	1
Nb Nb66	1	0.124232	0.923952	0.317082	1
Nb Nb67	1	0.375768	0.423952	0.682918	1

Nb Nb70 1 0.875768 0.076048 0.682918 1
 Nb Nb71 1 0.624232 0.576048 0.317082 1
 Nb Nb72 1 0.124232 0.423952 0.182918 1
 O O73 1 0.492806 0.746499 0.063384 1
 O O74 1 0.992806 0.253501 0.436616 1
 O O75 1 0.507194 0.753501 0.563384 1
 O O76 1 0.007194 0.246499 0.936616 1
 O O77 1 0.507194 0.253501 0.936616 1
 O O78 1 0.007194 0.746499 0.563384 1
 O O79 1 0.492806 0.246499 0.436616 1
 O O80 1 0.992806 0.753501 0.063384 1
 O O81 1 0.750463 0.910352 0.188317 1
 O O82 1 0.250463 0.089648 0.311683 1
 O O83 1 0.249537 0.589648 0.688317 1
 O O84 1 0.749537 0.410352 0.811683 1
 O O85 1 0.249537 0.089648 0.811683 1
 O O86 1 0.749537 0.910352 0.688317 1
 O O87 1 0.750463 0.410352 0.311683 1
 O O88 1 0.250463 0.589648 0.188317 1
 O O89 1 0.489415 0.751247 0.186705 1
 O O90 1 0.989415 0.248753 0.313295 1
 O O91 1 0.510585 0.748753 0.686705 1
 O O92 1 0.010585 0.251247 0.813295 1
 O O93 1 0.510585 0.248753 0.813295 1
 O O94 1 0.010585 0.751247 0.686705 1
 O O95 1 0.489415 0.251247 0.313295 1
 O O96 1 0.989415 0.748753 0.186705 1
 O O97 1 0.755704 0.912306 0.062871 1
 O O98 1 0.255704 0.087694 0.437129 1
 O O99 1 0.244296 0.587694 0.562871 1
 O O100 1 0.744296 0.412306 0.937129 1
 O O101 1 0.244296 0.087694 0.937129 1
 O O102 1 0.744296 0.412306 0.062871 1
 O O103 1 0.755704 0.412306 0.437129 1
 O O104 1 0.255704 0.587694 0.062871 1
 O O105 1 0.989415 0.248753 0.186705 1
 O O106 1 0.739808 0.153225 0.374913 1
 O O107 1 0.255704 0.087694 0.437129 1
 O O108 1 0.2(0.)9(65)-5(32)4(25)-5()6()- 0 0 1 206.57 275.09 Tm00.653225

O 0117 1 0.242748 0.842372 0.875237 1
O 0118 1 0.742748 0.157628 0.624763 1
O 0119 1 0.757252 0.657628 0.375237 1
O 0120 1 0.257252 0.342372 0.124763 1
O 0121 1 0.487412 0.018593 0.247209 1
O 0122 1 0.987412 0.981407 0.252791 1
O 0123 1 0.512588 0.481407 0.747209 1
O 0124 1 0.012588 0.518593 0.752791 1
O 0125 1 0.512588 0.981407 0.752791 1
O 0126 1 0.012588 0.018593 0.747209 1
O 0127 1 0.487412 0.518593 0.252791 1
O 0128 1 0.987412 0.481407 0.247209 1
O 0129 1 0.493081 0.238861 0.189072 1
O 0130 1 0.993081 0.761139 0.310928 1
O 0131 1 0.506919 0.261139 0.689072 1
O 0132 1 0.006919 0.738861 0.810928 1
O 0133 1 0.506919 0.761139 0.810928 1
O 0134 1 0.006919 0.238861 0.689072 1
O 0135 1 0.493081 0.738861 0.310928 1
O 0136 1 0.993081 0.261139 0.189072 1
O 0137 1 0.755456 0.161658 0.248569 1
O 0138 1 0.255456 0.838342 0.251431 1
O 0139 1 0.244544 0.338342 0.748569 1
O 0140 1 0.744544 0.661658 0.751431 1
O 0141 1 0.244544 0.838342 0.751431 1
O 0142 1 0.744544 0.161658 0.748569 1
O 0143 1 0.755456 0.661658 0.251431 1
O 0144 1 0.255456 0.338342 0.248569 1
O 0145 1 0.500000 0.000000 0.000000 1
O 0146 1 0.000000 0.000000 0.500000 1
O 0147 1 0.500000 0.500000 0.500000 1
O 0148 1 0.000000 0.500000 0.000000 1
O 0149 1 0.509289 0.253900 0.062752 1
O 0150 1 0.009289 0.746100 0.437248 1
O 0151 1 0.490711 0.246100 0.562752 1
O 0152 1 0.990711 0.753900 0.937248 1
O 0153 1 0.490711 0.746100 0.937248 1
O 0154 1 0.990711 0.253900 0.562752 1
O 0155 1 0.509289 0.753900 0.437248 1
O 0156 1 0.009289 0.246100 0.062752 1
O 0157 1 0.728666 0.181070 0.000347 1
O 0158 1 0.228666 0.818930 0.499653 1
O 0159 1 0.271334 0.318930 0.500347 1
O 0160 1 0.771334 0.681070 0.999653 1
O 0161 1 0.271334 0.818930 0.999653 1
O 0162 1 0.771334 0.181070 0.500347 1
O 0163 1 0.728666 0.681070 0.499653 1

O 070 1 0.498218 0.666480 0.801629 1
O 071 1 0.498105 0.664369 0.198059 1
O 072 1 0.498238 0.333700 0.802139 1
O 073 1 0.498468 0.997286 0.595980 1
O 074 1 0.498475 0.001069 0.404219 1
O 075 1 0.498016 0.497162 0.095988 1

Ba₃Nb₁₆O₂₃

_symmetry_space_group_name_H-M 'P 1'
_cell_length_a 4.23317500
_cell_length_b 12.66309700
_cell_length_c 21.30748300
_cell_angle_alpha 90.00022649
_cell_angle_beta 89.99923621
_cell_angle_gamma 89.99911484
_symmetry_Int_Tables_number 1
_chemical_formula_structural Ba₃Nb₁₆O₂₃
_chemical_formula_sum 'Ba₆ Nb₃₂ O₄₆'
_cell_volume 1142.18987747
_cell_formula_units_Z 2
loop_
_symmetry_equiv_pos_site_id
_symmetry_equiv_pos_as_xyz
1 'x, y, z'
loop_
_atom_site_type_symbol
_atom_site_label
_atom_site_symmetry_multiplicity
_atom_site_fract_x
_atom_site_fract_y
_atom_site_fract_z
_atom_site_occupancy
Ba Ba1 1 0.996455 0.000016 0.999922 1
Ba Ba2 1 0.998217 0.500675 0.499959 1
Ba Ba3 1 0.997041 0.000301 0.201349 1
Ba Ba4 1 0.997601 0.000231 0.798534 1
Ba Ba5 1 0.997651 0.500464 0.701363 1
Ba Ba6 1 0.997053 0.500554 0.298517 1
Nb Nb7 1 0.496530 0.327557 0.999963 1
Nb Nb8 1 0.496431 0.672401 0.999930 1
Nb Nb9 1 0.498117 0.828310 0.499937 1
Nb Nb10 1 0.498101 0.173153 0.499946 1
Nb Nb11 1 0.996413 0.329049 0.101486 1
Nb Nb12 1 0.996678 0.671085 0.898411 1
Nb Nb13 1 0.996320 0.671150 0.101449 1
Nb Nb14 1 0.996719 0.328996 0.898416 1
Nb Nb15 1 0.998249 0.829577 0.601462 1
Nb Nb16 1 0.997913 0.171739 0.398416 1
Nb Nb17 1 0.998224 0.171674 0.601488 1
Nb Nb18 1 0.997933 0.829638 0.398422 1
Nb Nb19 1 0.496339 0.500063 0.100993 1
Nb Nb20 1 0.496685 0.500000 0.898893 1
Nb Nb21 1 0.498275 0.000672 0.601001 1
Nb Nb22 1 0.497889 0.000720 0.398895 1

O 070 1 0.998147 0.840694 0.699380 1
O 071 1 0.997678 0.840783 0.300499 1
O 072 1 0.998186 0.160411 0.699397 1
O 073 1 0.996954 0.659935 0.800494 1
O 074 1 0.996544 0.340343 0.199395 1
O 075 1 0.996955 0.340244 0.800508 1
O 076 1 0.996453 0.660057 0.199370 1
O 077 1 0.496338 0.500259 0.201067 1
O 078 1 0.496845 0.500159 0.798815 1
O 079 1 0.498326 0.000494 0.701073 1
O 080 1 0.497860 0.000585 0.298822 1
O 081 1 0.496263 0.000122 0.103115 1
O 082 1 0.496696 0.000053 0.896717 1
O 083 1 0.498494 0.500621 0.603133 1
O 084 1 0.497931 0.500669 0.396786 1

BaNb₂O₆

_symmetry_space_group_name_H-M 'P 1'

_cell_length_a 5.96810002

_cell_length_b 8.06862644

O 023 1 0.151045 0.967329 0.287092 1
O 024 1 0.651083 0.030475 0.212108 1
O 025 1 0.654909 0.464715 0.213837 1
O 026 1 0.154757 0.532969 0.285507 1
O 027 1 0.352448 0.533061 0.785473 1
O 028 1 0.852428 0.464696 0.713819 1
O 029 1 0.494506 0.249297 0.647454 1
O 030 1 0.994630 0.748378 0.851843 1
O 031 1 0.512485 0.748482 0.351825 1
O 032 1 0.012747 0.249300 0.147375 1
O 033 1 0.613995 0.749793 0.637868 1
O 034 1 0.113981 0.247912 0.861271 1
O 035 1 0.393155 0.247999 0.361240 1
O 036 1 0.893360 0.749807 0.138018 1

Ba₃Nb₅O₁₅

_symmetry_space_group_name_H-M 'P 1'

_cell_length_a 4.05161200

_cell_length_b 12.85274900

_cell_length_c 12.85647601

_cell_angle_alpha 90.00058404

_cell_angle_beta 89.99766312

_cell_angle_gamma 90.00188315

_symmetry_Int_Tables_number 1

_chemical_formula_structural Ba₃Nb₅O₁₅

_chemical_formula_sum 'Ba₆ Nb₁₀ O₃₀'

_cell_volume 669.49265749

_cell_formula_units_Z 2

loop_

_symmetry_equiv_pos_site_id

_symmetry_equiv_pos_as_xyz

1 'x, y, z'

loop_

_atom_site_type_symbol

_atom_site_label

_atom_site_symmetry_multiplicity

_atom_site_fract_x

_atom_site_fract_y

_atom_site_fract_z

_atom_site_occupancy

Ba Ba1 1 0.997266 0.498912 0.499286 1

Ba Ba2 1 0.997152 0.998922 0.999326 1

Ba Ba3 1 0.998406 0.326327 0.836083 1

Ba Ba4 1 0.998052 0.671701 0.162551 1

Ba Ba5 1 0.996608 0.826648 0.662972 1

Ba Ba6 1 0.997047 0.171843 0.336332 1

Nb Nb7/F1 12 Tf5(3)7(2)-6()6(1)JTJET@0.51912 f5BT/F1 12 Tf1 0 0 1 271.61 333.65 Tm0 g0 G()JTJET@MC 21q

O 023 1 0.997501 0.419816 0.291393 1
O 024 1 0.997132 0.578012 0.707260 1
O 025 1 0.997154 0.919949 0.207318 1
O 026 1 0.997166 0.077862 0.791314 1
O 027 1 0.997238 0.706926 0.421387 1
O 028 1 0.997263 0.290879 0.577142 1
O 029 1 0.997104 0.790851 0.921522 1
O 030 1 0.997414 0.207053 0.077013 1
O 031 1 0.497021 0.155502 0.493289 1
O 032 1 0.497140 0.842203 0.505577 1
O 033 1 0.497591 0.655573 0.005535 1
O 034 1 0.497728 0.342296 0.993048 1
O 035 1 0.497858 0.506942 0.156183 1
O 036 1 0.497501 0.490870 0.842358 1
O 037 1 0.496845 0.990820 0.656203 1
O 038 1 0.496997 0.007153 0.342385 1
O 039 1 0.497493 0.357962 0.430800 1
O 040 1 0.497321 0.639601 0.567695 1
O 041 1 0.496963 0.858115 0.067794 1
O 042 1 0.497166 0.139711 0.930815 1
O 043 1 0.497235 0.565948 0.360726 1
O 044 1 0.497034 0.431857 0.637847 1
O 045 1 0.497229 0.931814 0.860726 1
O 046 1 0.497357 0.065997 0.137775 1

_symmetry_space_group_name_H-M 'P 1' Ca_8Al_3

AI AI21 1 0.676291 0.839839 0.025977 1
AI AI22 1 0.323709 0.160161 0.974023 1

AI

Al

_symmetry_space_group_name_H-M 'P 1'
_cell_length_a 2.85042097
_cell_length_b 2.85042097
_cell_length_c 2.85042097
_cell_angle_alpha 60.00000000
_cell_angle_beta 60.00000000
_cell_angle_gamma 60.00000000
_symmetry_Int_Tables_number 1

CaAl₄

_symmetry_space_group_name_H-M 'P 1'
_cell_length_a 6.39847767
_cell_length_b 6.39847767
_cell_length_c 6.39847767
_cell_angle_alpha 140.30519444
_cell_angle_beta 140.30519444
_cell_angle_gamma 57.39019638
_symmetry_Int_Tables_number 1
_chemical_formula_structural CaAl₄
_chemical_formula_sum 'Ca1 Al4'
_cell_volume 105.95058245
_cell_formula_units_Z 1
loop_
_symmetry_equiv_pos_site_id
_symmetry_equiv_pos_as_xyz
1 'x, y, z'
loop_
_atom_site_type_symbol
_atom_site_label
_atom_site_symmetry_multiplicity
_atom_site_fract_x
_atom_site_fract_y
_atom_site_fract_z
_atom_site_occupancy

CaAl₂

_symmetry_space_group_name_H-M 'P 1'
_cell_length_a 5.66432978
_cell_length_b 5.66432978
_cell_length_c 5.66432978
_cell_angle_alpha 60.00000000
_cell_angle_beta 60.00000000
_cell_angle_gamma 60.00000000
_symmetry_Int_Tables_number 1
_chemical_formula_structural CaAl₂
_chemical_formula_sum 'Ca₂ Al₄'
_cell_volume 128.50812690
_cell_formula_units_Z 2
loop_
_symmetry_equiv_pos_site_id
_symmetry_equiv_pos_as_xyz
1 'x, y, z'
loop_

CaO

CaAl₄O₇

```
_symmetry_space_group_name_H-M 'P 1'  
_cell_length_a 7.87908043  
_cell_length_b 7.87908043  
_cell_length_c 5.49135228  
_cell_angle_alpha 76.63155928  
_cell_angle_beta 76.63155928  
_cell_angle_gamma 69.28149864  
_symmetry_Int_Tables_number 1  
_chemical_formula_structural CaAl4O7  
_chemical_formula_sum 'Ca2 Al8 O14'  
_cell_volume 306.00622724  
_cell_formula_units_Z 2  
loop_  
_symmetry_equiv_pos_site_id  
_symmetry_equiv_pos_as_xyz  
1 'x, y, z'  
loop_  
_atom_site_type_symbol  
_atom_site_label  
_atom_site_symmetry_multiplicity  
_atom_site_fract_x  
_atom_site_fract_y  
_atom_site_fract_z  
_atom_site_occupancy  
Ca Ca1 1 0.804883 0.195117 0.250000 1  
Ca Ca2 1 0.195117 0.804883 0.750000 1  
Al Al3 1 0.319417 0.439886 0.243609 1  
Al Al4 1 0.560114 0.680583 0.256391 1  
Al Al5 1 0.680583 0.560114 0.756391 1  
Al Al6 1 0.439886 0.319417 0.743609 1  
Al Al7 1 0.922581 0.751201 0.305795 1  
Al Al8 1 0.248799 0.077419 0.194205 1  
Al Al9 1 0.077419 0.248799 0.694205 1  
Al Al10 1 0.751201 0.922581 0.805795 1  
O O11 1 0.251362 0.362711 0.579734 1  
O O12 1 0.637289 0.748638 0.920266 1  
O O13 1 0.748638 0.637289 0.420266 1  
O O14 1 0.362711 0.251362 0.079734 1  
O O15 1 0.135780 0.627911 0.149387 1  
O O16 1 0.372089 0.864220 0.350613 1  
O O17 1 0.864220 0.372089 0.850613 1  
O O18 1 0.627911 0.135780 0.649387 1
```

O 023 1 0.829950 0.939148 0.072687 1
O 024 1 0.060852 0.170050 0.427313 1

AI	AI23	1	0.534143	0.500000	0.000000	1
AI	AI24	1	0.500000	0.000000	0.534143	1
AI	AI25	1	0.000000	0.534143	0.500000	1
AI	AI26	1	0.965857	0.965857	0.965857	1
O	O27	1	0.500000	0.000000	0.867850	1
O	O28	1	0.867850	0.500000	0.000000	1
O	O29	1	0.000000	0.867850	0.500000	1
O	O30	1	0.632150	0.632150	0.632150	1
O	O31	1	0.367850	0.500000	0.000000	1
O	O32	1	0.500000	0.000000	0.367850	1
O	O33	1	0.000000	0.367850	0.500000	1
O	O34	1	0.132150	0.132150	0.132150	1
O	O35	1	0.408850	0.094214	0.615227	1

Ca₁₁Al₁₄O₃₂

_symmetry_space_group_name_H-M 'P 1'
_cell_length_a 12.04438581
_cell_length_b 12.08491300
_cell_length_c 12.15689086
_cell_angle_alpha 90.00000000
_cell_angle_beta 89.95748726
_cell_angle_gamma 90.00000000
_symmetry_Int_Tables_number 1
_chemical_formula_structural Ca₁₁Al₁₄O₃₂
_chemical_formula_sum 'Ca₂₂ Al₂₈ O₆₄'
_cell_volume 1769.50007290
_cell_formula_units_Z 2
loop_
_symmetry_equiv_pos_site_id
_symmetry_equiv_pos_as_xyz
1 'x, y, z'
loop_
_atom_site_type_symbol
_atom_site_label
_atom_site_symmetry_multiplicity
_atom_site_fract_x
_atom_site_fract_y
_atom_site_fract_z
_atom_site_occupancy

AI AI23 1 0.250000 0.378655 0.000000 1
AI AI24 1 0.750000 0.125653 0.000000 1
AI AI25 1 0.997795 0.249086 0.374848 1
AI AI26 1 0.001875 0.748966 0.125332 1
AI AI27 1 0.373889 0.999505 0.248917 1
AI AI28 1 0.126111 0.999505 0.751083 1
AI AI29 1 0.763486 0.266993 0.226260 1
AI AI30 1 0.236071 0.766877 0.273715 1
AI AI31 1 0.267560 0.233312 0.767443 1
AI AI32 1 0.232440 0.233312 0.232557 1
AI AI33 1 0.980823 0.016757 0.517770 1
AI AI34 1 0.019321 0.516697 0.982398 1
AI AI35 1 0.517159 0.983390 0.016809 1
AI AI36 1 0.482791 0.483489 0.483029 1
AI AI37 1 0.750000 0.878898 0.500000 1
AI AI38 1 0.250000 0.625649 0.500000 1
AI AI39 1 0.498125 0.748966 0.874668 1
AI AI40 1 0.502205 0.249086 0.625152 1
AI AI41 1 0.874182 0.499652 0.749039 1
AI AI42 1 0.625818 0.499652 0.250961 1
AI AI43 1 0.263929 0.766877 0.726285 1
AI AI44 1 0.736514 0.266993 0.773740 1
AI AI45 1 0.767168 0.733328 0.267470 1
AI AI46 1 0.732832 0.733328 0.732530 1
AI AI47 1 0.480679 0.516697 0.017602 1
AI AI48 1 0.519177 0.016757 0.482230 1
AI AI49 1 0.017209 0.483489 0.516971 1
AI AI50 1 0.982841 0.983390 0.983191 1
O O51 1 0.161130 0.685366 0.780854 1
O O52 1 0.839571 0.185518 0.719564 1
O O53 1 0.685089 0.813243 0.180451 1
O O54 1 0.314534 0.313191 0.319593 1
O O55 1 0.065747 0.935567 0.431598 1
O O56 1 0.934323 0.435492 0.068557 1
O O57 1 0.433580 0.068541 0.935599 1
O O58 1 0.066420 0.068541 0.064401 1
O O59 1 0.140786 0.448587 0.937383 1
O O60 1 0.359214 0.448587 0.062617 1
O O61 1 0.650831 0.034504 0.055681 1
O O62 1 0.349081 0.534514 0.444171 1
O O63 1 0.689069 0.217509 0.905388 1
O O64 1 0.311099 0.717400 0.594556 1
O O65 1 0.305280 0.286557 0.899479 1
O O66 1 0.194720 0.286557 0.100521 1
O O67 1 0.956156 0.150633 0.468739 1
O O68 1 0.056183 0.355291 0.456224 1
O O69 1 0.044061 0.650548 0.031595 1

Ca₂₃Al₂₈O₆₄

_symmetry_space_group_name_H-M 'P 1'
_cell_length_a 12.07214259
_cell_length_b 12.09020809
_cell_length_c 12.12961665
_cell_angle_alpha 90.00000000
_cell_angle_beta 89.99195483
_cell_angle_gamma 90.00000000
_symmetry_Int_Tables_number 1
_chemical_formula_structural Ca₂₃Al₂₈O₆₄
_chemical_formula_sum 'Ca₂₃ Al₂₈ O₆₄'
_cell_volume 1770.37473638
_cell_formula_units_Z 1
loop_
_symmetry_equiv_pos_site_id
_symmetry_equiv_pos_as_xyz
1 'x, y, z'
loop_
_atom_site_type_symbol
_atom_site_label
_atom_site_symmetry_multiplicity
_atom_site_fract_x
_atom_site_fract_y
_atom_site_fract_z
_atom_site_occupancy
Ca Ca1 1 0.250000 0.639453 -0.000000 1
Ca Ca2 1 0.250000 0.363106 0.500000 1
Ca Ca3 1 0.250000 0.887496 0.500000 1
Ca Ca4 1 0.250000 0.111280 -0.000000 1
Ca Ca5 1 0.995768 0.244617 0.633740 1
Ca Ca6 1 0.504232 0.244617 0.366260 1
Ca Ca7 1 0.500027 0.250835 0.885660 1
Ca Ca8 1 0.999973 0.250835 0.114340 1
Ca Ca9 1 0.634996 0.002980 0.253318 1
Ca Ca10 1 0.362710 0.498329 0.250523 1
Ca Ca11 1 0.887005 0.498802 0.251662 1
Ca Ca12 1 0.112268 0.000654 0.251396 1
Ca Ca13 1 0.750000 0.864140 -0.000000 1
Ca Ca14 1 0.750000 0.389214 -0.000000 1
Ca Ca15 1 0.750000 0.617536 0.500000 1
Ca Ca16 1 0.499919 0.750962 0.136514 1
Ca Ca17 1 0.000081 0.750962 0.863486 1
Ca Ca18 1 0.998442 0.752778 0.388771 1
Ca Ca19 1 0.501558 0.752778 0.611229 1
Ca Ca20 1 0.137290 0.498329 0.749477 1
Ca Ca21 1 0.865004 0.002980 0.746682 1
Ca Ca22 1 0.387732 0.000654 0.748604 1

O 070 1 0.056162 0.651326 0.034493 1
O 071 1 0.444027 0.354197 0.541412 1
O 072 1 0.899168 0.692227 0.214141 1
O 073 1 0.605362 0.302827 0.713907 1
O 074 1 0.894638 0.302827 0.286093 1 Tf1 0 0 1 59.52 597.34 Tm0 g0 G(O On./F1 12 582.65 0 0 1 59.52 6
O 075 1 0.097627 0.195947 0.282170 1
O 076 1 0.463199 0.943609 0.148553 1
O 077 1 0.461067 0.052988 0.350196 1
O 078 1 0.038933 0.052988 0.649804 1
O 079 1 0.536002 0.443321 0.350402 1
O 080 1 0.216042 0.899422 0.694462 1
O 081 1 0.00008871 0 595.32 848841.92 re08227 0.214141 1

Ag

AlAg

_symmetry_space_group_name_H-

1. Zhang, X., Zhang, L., Perkins, J. D., and Zunger, A., (2015), Intrinsic transparent conductors without doping. *Phys. Rev. Lett.*, 115, 176602.
2. Kummer, J. T., (1972), γ -Alumina electrolytes. *Prog. Solid State Chem.*, 7, 141-175.2 7
3. England, W. A., Jacobson, A. J., and Tofield, B. C., (1982), Structural studies of highly non-stoichiometric polycrystalline sodium and silver beta-aluminas. *Solid State Ion.*, 6, 21-27.
4. Iyi, N., Inoue, Z., and Kimura, S., (1986), The crystal structure of highly nonstoichiometric potassium γ -alumina, $K_{1.50}Al_{11.0}O_{17.25}$. *J. Solid State Chem.*, 61, 81-89.
- 5.3 Van Berkel, F. P. F., Zandbergen, H. W., Verschoor, G. C., and IJdo, D. J. W., (1984), The structure of barium aluminate $Ba_{0.95}Al_{11}O_{17.25}$. *Acta Cryst.*, B40, 198